Applied Physics Letters

Ultrasonic evaluation of aging kinetics in amorphous polymer

Cite as: Appl. Phys. Lett. **121**, 072202 (2022); https://doi.org/10.1063/5.0102398
Submitted: 09 June 2022 • Accepted: 29 July 2022 • Published Online: 17 August 2022
Published open access through an agreement with JISC Collections

P. Yambangyang, R. Wilson, J. Reboud, et al.

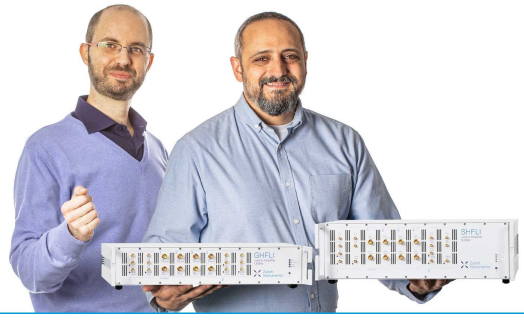

Applied Physics Letters ARTICLE scitation.org/journal/apl

Ultrasonic evaluation of aging kinetics in amorphous polymer

Cite as: Appl. Phys. Lett. **121**, 072202 (2022); doi: 10.1063/5.0102398
Submitted: 9 June 2022 · Accepted: 29 July 2022 ·
Published Online: 17 August 2022

P. Yambangyang,[1] R. Wilson,[2] J. Reboud,[2] J. M. Cooper,[2] and A. Demčenko[2,a)]

AFFILIATIONS

[1]Faculty of Engineering, Mahidol University, Bangkok 73210, Thailand
[2]Division of Biomedical Engineering, James Watt School of Engineering, The University of Glasgow, Rankine Building, Oakfield Avenue, Glasgow G12 8LT, United Kingdom

[a)]Author to whom correspondence should be addressed: Andriejus.Demcenko@glasgow.ac.uk

ABSTRACT

The physical aging of amorphous polymers induces changes in material properties, which are challenging to detect *in situ* in industrial settings. Here, we present a nondestructive nonlinear ultrasonic evaluation technique that enables localized measurements of the combined effects of temperature and time in amorphous polymers, without needing to remove materials. The proposed technique is demonstrated using commercial grade poly(vinyl chloride) samples and is supported by analysis of wave–material interactions. The results show that the physical aging of the polymer is described by the Arrhenius equation with an effective activation energy of 103 kJ/mol over the analyzed temperature range.

Amorphous solids are used widely in applications including pharmacy,[1,2] healthcare,[3] structural engineering, and industrial manufacturing,[4–6] giving rise to a significant interest in characterizing their stability over time. It is already known that such solids undergo slow structural relaxations, which are commonly described as physical aging.[1,7–9] This relaxation does not require any external stimulus, in contrast to phenomena involved in mechanical, chemical, and photo-chemical aging. However, these small changes (for example, less than 0.2% change in volumetric mass density of polystyrene, see Ref. 10) in materials' properties are difficult to detect[11] *in situ* in industrial settings, using conventional nondestructive techniques, such as ultrasound in a linear regime.[12] Our work, here, now focuses on the development of a nonlinear ultrasonic evaluation technique, which we demonstrate by measuring the physical aging of the thermoplastic polymer, poly(vinyl chloride) (PVC), commonly used in bulk,[6,13–15] as a visco-hyper-elastic isotropic amorphous polymer for pipes.[16]

A temperature interval bounded by T_β and T_g describes the range over which physical aging occurs,[17,18] see Fig. S1 of the supplementary material, where T_β and T_g are the beta and glass transition temperatures, respectively. It has also been shown that physical aging is possible below T_β,[19] the relaxation transition closest to the glass transition temperature T_g of the polymer. The aging process within this regime is governed by the Arrhenius equation[6,18] given by $K(T) = Ae^{-E_a/RT}$, where A is the pre-exponential factor, $K(T)$ is the rate of the process, T is the absolute temperature for the process, E_a is the activation energy, and R is the universal gas constant. Below T_β, all secondary motion is frozen in polymers.[17]

In the case of PVC, $T_\beta \approx -50\,^\circ$C,[7] while T_g is in the range of 80 °C.[20,21] By knowing the activation energy E_a for such a polymer, the Arrhenius equation enables us to predict the combined effect of temperature and time for first-order kinetics.[6]

Previously, single values of the activation energy have been reported for the physical aging of PVC.[22–24] Vyazovkin *et al.*[25] discusses ranges of PVC's activation energy, indicating that its estimation depends upon a number of factors including material composition, the criterion monitored, and experimental factors, including the estimation methods used.[26]

Historically, such estimation methods comprised only laboratory techniques,[9] with limited applicability in industrial and field settings, requiring complex instrumentation where analyses must be performed *ex situ*. For example, differential scanning calorimetry (DSC) is one of the principal sources of T_g data for many types of materials,[1] used to characterize physical aging. However, this technique is not performed in industrial or field settings, as it requires that each discrete data point is collected after a specific

period of aging, to give an experimental measure of the enthalpy recovery.[27]

Here, we now propose an ultrasonic evaluation technique, which is truly nondestructive, enabling us to characterize physical aging in amorphous thermoplastic polymers without *a priori* knowledge of the material's thermohistory. The technique is based on nonlinear ultrasonics, which has previously been shown to be sensitive to time of polymer annealing, using both laboratory and field specimens.[12,28] In this work, which goes beyond the transmission mode used previously[12] and also allows pulse-echo modes, we now demonstrate a technique that enables not only detection but also activation energy measurement. Our methodology is suitable for measurements performed in laboratory conditions but can also be used for localized evaluation of physical aging in thermoplastic polymers in the field and in industrial settings including curved/cylindrical geometries,[12] without sampling or cutting specimens from engineering structures, after a simple reconfiguration of the transducer geometries. The technique can also be carried out for specific spatial volumes on the order of cubic millimeters, through the thickness of a given engineering structure, enabling us to measure the effective activation energy *in situ* E_a, thus defining the physical aging rate. In a similar way as for ellipsometry-based techniques,[27] this nonlinear ultrasonic method also allows continuous monitoring of physical aging.

Our nondestructive technique is implemented in the following three steps, involving: first, the measurement of the initial state of the polymer; second, localized rejuvenation of the polymer or estimation of baseline properties; and finally, the measurement of the polymer response without thermal history.

The first and third steps are identical except that the ultrasonic responses from the specimen are measured before and after the erasure of the thermal history (step 2).

It has previously been shown that nonlinear ultrasonics is more sensitive to physical aging than linear ultrasound.[12,28] We use a classical parametric wave mixing method[29,30] based upon the interaction of two initial waves. The classical wave mixing conditions fulfill the laws of momentum and energy conservation, accordingly,

$$\begin{aligned} \mathbf{k} &= \mathbf{k_1} \pm \mathbf{k_2}, \\ \omega &= \omega_1 \pm \omega_2, \end{aligned} \tag{1}$$

where $\mathbf{k}$ is the wave vector at the combined frequency with the corresponding wavenumber $k = 2\pi(f_1 \pm f_2)/c$, c is the nonlinear wave velocity, $\mathbf{k}_{1,2}$ are the wave vectors of two initial waves with the corresponding wavenumbers $k_{1,2} = 2\pi f_{1,2}/c_{1,2}$, and $c_{1,2}$ are the longitudinal $c_l = \sqrt{(\lambda + 2\mu)/\rho}$ or transverse $c_t = \sqrt{2\mu/\rho}$ wave velocities of the interacting waves. $\omega = 2\pi(f_1 \pm f_2)$ and $\omega_{1,2} = 2\pi(f_{1,2})$ are the angular frequencies of the nonlinear and initial waves, respectively. These resonance conditions enable us to calculate the angle α between two interacting waves for the selected frequencies. Figure 1 shows an example that depicts a submerged ultrasonic setup, as would be required for inspection of water mains piping, analyzed by using parametric wave mixing. We consider ultrasonic signals at the sum frequency. In this report, for completeness, we demonstrated both the pulse-echo (receiver R_1) and through-transmission (receiver R_2) measurement modes. The pulse-echo mode requires only single-side access of the sample, utilizing the reflection from the bottom surface, which is advantageous in *in situ* industrial settings where measurements are

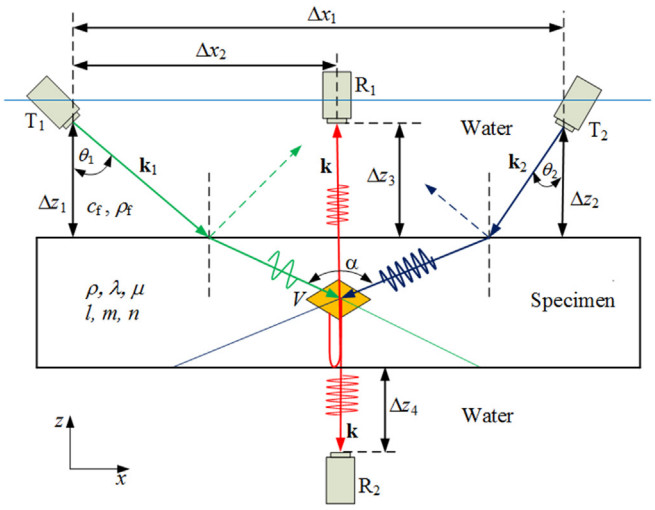

FIG. 1. Measurement setup and coordinate system for parametric wave mixing in submersion ultrasonics, using classical nonlinear wave interactions for localized contactless sensing within the volume V. α is the interaction angle between the two waves excited by sources T_1 and T_2. This configuration only requires planar alignment of the transducers, which is carried out manually here but could be automated with a phased array (for example, see Sec. SIII of the supplementary material).

being made in the field, e.g., evaluating the integrity of pipes from their inner side using a mobile autonomous device.[31]

The intensity of the nonlinear ultrasonic signal depends upon the linear (λ and μ) and nonlinear (l, m, and n in Murnaghan notation[32]) elastic material properties, as well as upon the interaction volume V. Using submersion ultrasonics, as might be required for pipe inspection, and employing the classical wave interactions at the sum frequency, the polymer's physical aging was evaluated from changes in the third order elastic constant m only.[29] The remaining two elastic constants l and n are not involved in the nonlinear interaction for the parametric wave mixing configuration selected, allowing other configurations for sensing of other phenomena simultaneously.

The sensitivity of the physical aging changes observed in the nonlinear mode contrasts greatly with that obtained using linear elastic properties (where the very small changes in λ, μ, and the volumetric mass density ρ greatly limit the measurement methods).[12,28,33]

The simplest way to estimate the thermohistory of a polymer is to measure the response from an un-aged specimen as a reference. However, it is practically impossible to maintain engineering structures or their parts in the un-aged state or uniformly aged at controlled conditions. Consequently, samples from different parts of the structure under study are often rejuvenated.

In the practical implementation of construction and maintenance of engineered structures, objects contain elements made by different factories, which use different recipes and conditions in their production of polymer elements, so samples of materials must be obtained from all non-identical parts. Sampling from the surface of an object can often be readily performed, but these samples generally do not represent the actual system with high fidelity, as they interact with the surrounding environment or/and atmospheric conditions,[34,35] leading to limited insight (as is the case for microindentation hardness evaluation[36]). For example, aging rates are different in the bulk of the

material, compared to its surfaces (see Ref. 10). To minimize the influence of uncontrolled conditions, specimens below surfaces are preferable, but sampling these from the bulk is usually detrimental to the structure's integrity.

Here, we demonstrate a localized acoustic rejuvenation method for the estimation of the baseline thermohistory of the polymer. This draws upon our knowledge that the viscoelasticity of an amorphous polymer enables efficient transfer of acoustic energy to heat, without direct contact between the ultrasonic transducer and specimen. Moreover, such ultrasonic heating can be controlled both spatially and temporally without damaging the polymer specimens.[37] Figure 2 shows such an ultrasonic setup for the localized rejuvenation of thermoplastic polymers, where a spherically focused transducer is used to generate longitudinal waves which heat the polymer above T_g. The heated material below T_g experiences an "accelerated" aging at the increased temperature, although, over the short duration of active heating, such processes were negligible and were discounted (in our work, $t_{\text{heating}} = 10$ s).

The interaction between the polymer and ultrasound leads to absorption of the longitudinal waves, which depends upon[38] (1) subchain motions between polymer chain entanglements generally described by "Rouse"-like motions and (2) entanglement effects which become dominant in a low frequency range ($\lesssim$1 MHz). The heat is generated from viscous sliding and shearing of polymer chains at the molecular level.[39]

The temperature profile as a function of time can be analyzed using the following equation:[40,41]

$$\rho C \frac{\partial T}{\partial t} = \kappa \nabla^2 T + Q, \tag{2}$$

where C is the specific heat capacity, t is the time, κ is the thermal conductivity, Q is the heat generation due to the viscous absorption of ultrasound which, for a monochromatic or quasi-monochromatic wave with a center frequency f_0, is[40,42]

$$Q = 2\alpha(f_0, T) I(T), \tag{3}$$

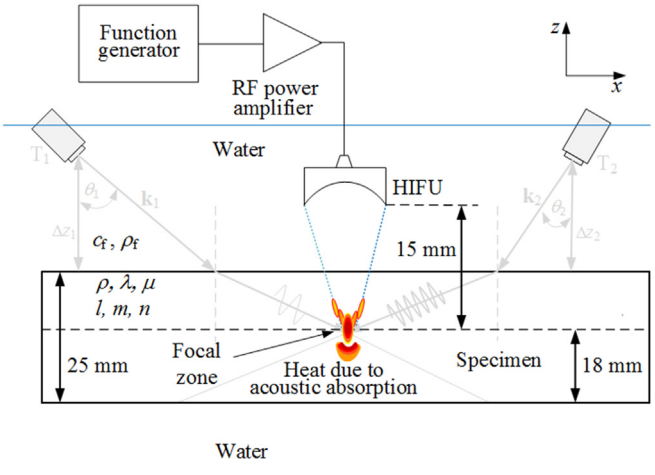

FIG. 2. Schematic diagram of the experimental setup for localized ultrasonic rejuvenation of thermoplastic polymers using a spherically focused transducer which generated high intensity focused ultrasound (HIFU).

where $\alpha(f_0, T)$ is the wave attenuation coefficient at the frequency f_0 and temperature T, and $I(T)$ is the temperature dependent wave intensity[43]

$$I(T) = 2\pi^2 f_0^2 \rho(T) c(f_0, T) |u_0|^2, \tag{4}$$

where $c(f_0, T)$ is the wave velocity and u_0 is the amplitude of wave displacement.

Equation (3) shows that the heat generation depends upon material parameters (including the wave velocity, its attenuation, and the volumetric material density) which are all temperature dependent.[42,44,45] It is already known that the attenuation of ultrasound waves increases with temperature, so the polymer heating becomes more efficient at higher temperatures (see Ref. 42). This enables an efficient rejuvenation of the polymer, above T_g. It is useful to note that the system allows for other sources for heating (e.g., a laser). However, such configurations would need further alignment that is not required when using ultrasound.

In polymers, the first-order kinetics[6] depend upon the activation energy E_a that can be calculated as the gradient of the Arrhenius coordinates.[46]

Given the dependence of the physical aging rate upon temperature T, isothermal measurements of an ultrasonic response at different temperatures, see Fig. S2 of the supplementary material, enable us to create an experimental master curve, which shows the aging rate vs temperature. The activation energy is found by minimizing the following objective function:

$$\min\left(\frac{1}{2}\sum \left(\mathbf{K}(T) - \mathbf{K}_e(T)\right)^2\right), \tag{5}$$

where $\mathbf{K}_e(T)$ is the measured aging rate (proportional to the third order elastic constant m).

Experimental conditions, configuration of the setup, and material properties are presented in Sec. SIII of the supplementary material.

Figure 3 shows amplitude C-scan images from nonlinear and linear ultrasonic measurements in the pulse-echo and through-transmission modes, when a localized ultrasonic rejuvenation was used to erase the thermal history of PVC specimens. The amplitude of the nonlinear ultrasonic signal was calculated from filtered signals. A finite impulse response narrow-band bandpass filter with a center frequency at 5 MHz was used to process the signals. The data were normalized for each experiment individually, in order to compare experimental results, using the following expression:

$$\mathbf{A} = \frac{\mathbf{A}_0 - \min(\mathbf{A}_r)}{\max(\mathbf{A}_r) - \min(\mathbf{A}_r)}, \tag{6}$$

where $\mathbf{A}_0$ is the peak-to-peak amplitude matrix of the whole C-scan data, $\mathbf{A}_r$ is the reference peak-to-peak amplitude data of the C-scan, excluding the locally rejuvenated area. The normalization with respect to the background (non-rejuvenated area) enables us to highlight variations of the ultrasonic signals for the different experiments.

The results show a complex ultrasonic response, see Figs. 3(a)–3(c), in which the linear through-transmission experiment results represent the simplest amplitude of the ultrasonic signal distribution in the specimen, see Fig. 3(d), as in agreement with the previously reported results. The amplitude of the linear signal decreased due to the rejuvenation of PVC.[28] The C-scan image shows that a vertical

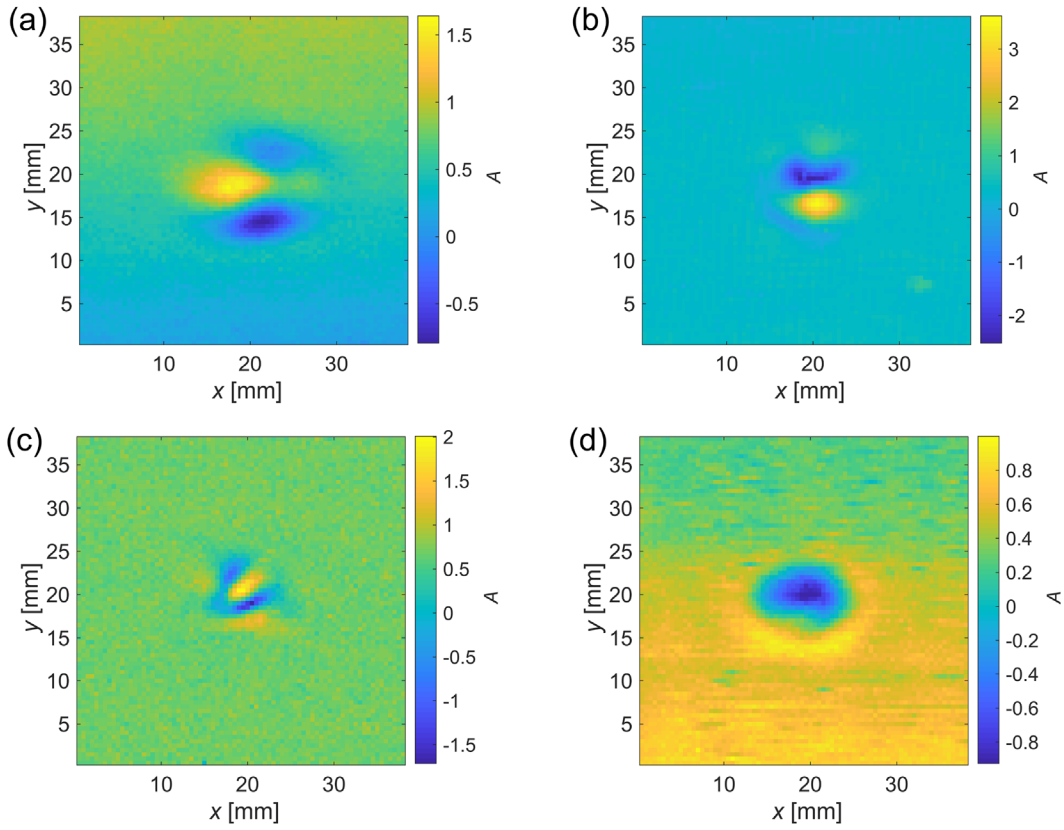

FIG. 3. Amplitude C-scan images of locally rejuvenated PVC specimens: nonlinear ultrasonic experiments in the pulse-echo (a) and through-transmission (b) modes and linear ultrasonic measurements in the pulse-echo (c) and through-transmission modes (d).

projection of the locally rejuvenated volume, which acts as a shadow for the ultrasonic signals, is close to circle. This is in good agreement with a thermogram, see Fig. S5 of the supplementary material, which shows a peak temperature $T = 50\,^{\circ}$C on the surface of the specimen after it is removed from water.

In the pulse-echo mode, see Fig. 3(a), the signs of the amplitudes are inversed, so an increase in the amplitude must be considered in the evaluation of the physical aging in PVC, while it is given as a decrease in the through-transmission experiments [see Fig. 3(b)]. In the nonlinear ultrasonic experiments, the locally rejuvenated volume serves as an inhomogeneity with a boundary, which acts as an interface between the rejuvenated and non-rejuvenated media. During the scanning measurements, the boundary of the rejuvenated volume is partially included inside the interaction volume V, see Fig. 1, for each scanning position, making nonlinear interactions between the two initial waves weaker, resulting in the decrease in the signal amplitudes as seen in Fig. 3(a). The nonlinear interactions under imperfect resonance conditions are discussed in Ref. 47.

The linear ultrasonic pulse-echo mode results depicted in Fig. 3(c) show sharp changes in the signals amplitudes (see Fig. S6 of the supplementary material for the signals). Assuming a spherical shape for the locally rejuvenated volume, see Fig. 4, when the ultrasonic transducer is positioned above an apex of the sphere, the sphere serves as a double lens for the ultrasonic waves. In this case, the ultrasonic signals have a higher amplitude. When the transducer is pointing to a side of the sphere, the beam divergence results in higher losses, generating ultrasonic signals with lower amplitudes. The results depicted in the C-scan image [Fig. 3(c)] do not show the symmetric circular distribution of the amplitudes that is expected for a spherical volume due to the complex shape of the rejuvenated volume.

Figure 5 shows C-scan images after rejuvenation of the polymer specimen in the furnace ($T = 90\,^{\circ}$ C and $t = 1$ h) and quenching in the antifreeze fluid ($T = -34\,^{\circ}$ C). The results do not contain residuals of the localized rejuvenation, confirming a thorough erasure of the thermal history using the ultrasonic waves. Note that heating and quenching of the polymer induce residual stresses in specimens[48,49] which could also affect ultrasonic response from the materials. The potential impact of residual stress in PVC was examined employing an acoustoelasticity analysis.[50] When the residual stress $\sigma_{11} = 10$ MPa,[6] the maximum wave velocity changes are 30 and 5 m/s for the longitudinal and transverse (vertical polarization) waves, respectively. These changes are dependent on the wave propagation direction. The limited impact of residual stress is also consistent with the fact that time-of-flight ultrasonic signals do not indicate any localized variation (see Fig. S7 in the supplementary material).

The nonlinear ultrasonic responses from rejuvenated and quenched PVC specimens were measured at three different annealing temperatures: 24, 26, and 28 °C. The measurements were performed

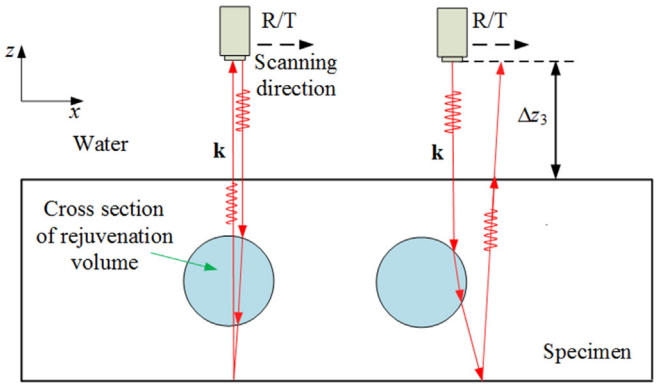

FIG. 4. Representation of pulse-echo ultrasonic wave propagation through the locally rejuvenated volume in the polymer, in the model case where the volume is spherical.

at 5 s sampling rate, and three measurements were conducted at each temperature point. The ultrasonic signals were filtered using a finite impulse response narrow-band bandpass filter with a center frequency at 6.25 MHz. The energy of the filtered signals was calculated from the experimental data, to estimate the gradient (Fig. S2 of the supplementary material).

Experimental gradients at the different temperatures are listed in Table I. The activation energy E_a was calculated by minimizing the objective function presented in Eq. (5), as 103 kJ/mol. The coefficient of determination of the data plot in the Arrhenius coordinates is 0.999, providing confidence in the experimental results. A Monte Carlo analysis was used to estimate standard deviation of the result. 10M iterations were made varying randomly the gradient values within a range of the mean value of the standard deviations listed in Table I. A normal distribution was assumed in the analysis. The analysis shows that the standard deviation of the effective activation energy is ±46 kJ/mol. The measured value is consistent with reported results[21] which show that the energy E_a varies in the range of 60–150 kJ/mol, while the actual value depends on multiple factors.[26]

We propose that future experimental work may involve exploring reference methods that corroborate our measured values although we also note that at present the standardization of current techniques[21–24] present challenges in providing reproducible reference measurements. Our long-term aim is to position our methodology as the gold-standard within the suite of analytical technique used to characterize polymer aging.

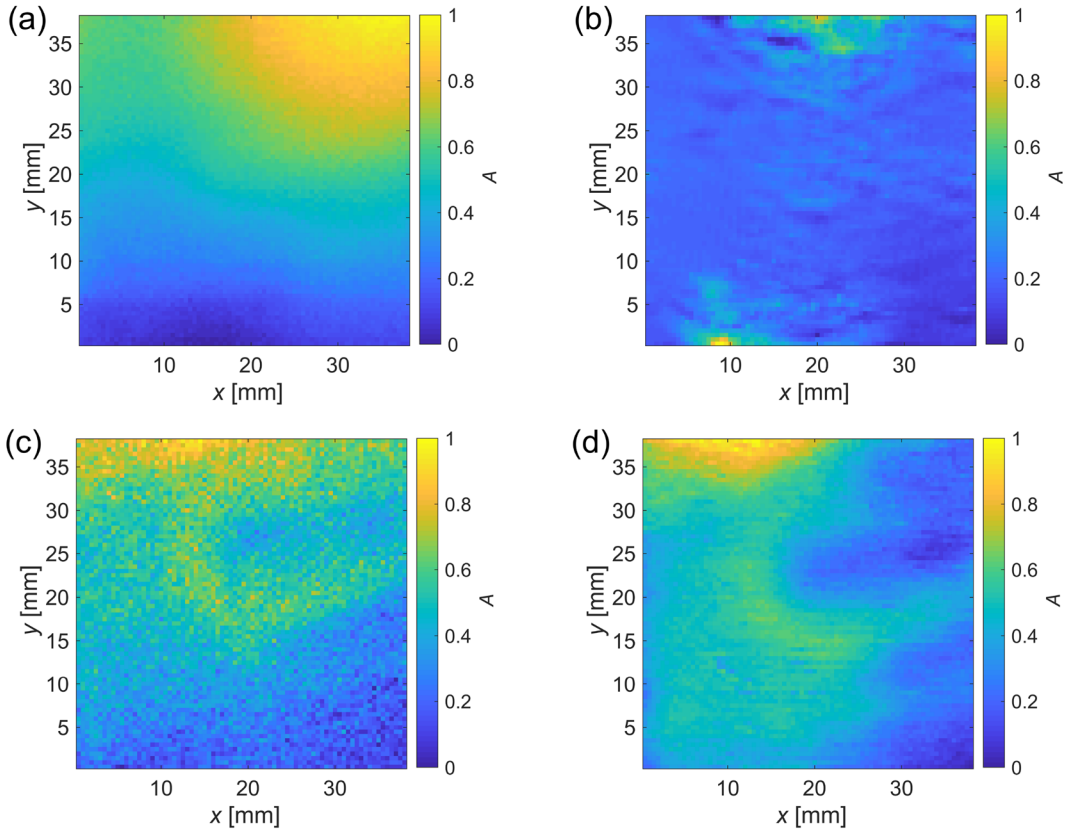

FIG. 5. Amplitude C-scan images of fully rejuvenated PVC specimens: nonlinear ultrasonic experiments in the pulse-echo (a) and through-transmission (b) modes and linear ultrasonic measurements in the pulse-echo (c) and through-transmission modes (d). The amplitude variations of ultrasonic signals are due to the small inclination of the specimen.

TABLE I. Results of the isothermal measurements, where ± shows the standard deviation from three experiments at each measurement temperature.

Temperature (°C)	24	26	28
Gradient	4.314 ± 0.328	5.982 ± 0.204	8.166 ± 0.445

A truly nondestructive, ultrasonic evaluation technique for the measurement of physical aging in amorphous thermoplastic polymers was presented in this study. In contrast to other methods used to sense physical aging, our technique enables localized *in situ* evaluation of polymers both in laboratory and industrial settings without the need for cutting specimens from engineering structures. The proposed nonlinear ultrasonic method was used to evaluate the combined effect of temperature and time on the first-order kinetics of commercial grade PVC specimens, showing that (i) physical aging is governed by the activation energy (measured as 103 kJ/mol in the temperature range of 24–28 °C) and that (ii) the process is described by the Arrhenius equation.

Our technique has the potential to recover temporal information from thermoplastic polymers when in-service conditions are known or controlled. This information is extremely valuable for prognostic maintenance and health monitoring of engineering infrastructure, leading to more sustainable processes.

Our proposed ultrasonic rejuvenation technique can not only erase the thermohistory of polymers but it could also be used to form composite structures from a bulk monolithic material. For example, layered structures can be formed at specific zones of engineering infrastructure components to maintain desired properties and could also be structured into phononic lattices encoded into the infrastructure to enhance structure health monitoring signals.

In the future, our technique could be used to enable explorations of acoustic interaction with amorphous polymers and soft tissues (such as living cells in microfluidic systems)[51–55] including their nonlinear responses. This could open new applications complementing methods such as differential scanning calorimetry, to understand spatial distribution of material properties, by using a locally rejuvenated volume of the polymer.

See the supplementary material for free volume concept, isothermal nonlinear ultrasonic response, experimental conditions and material properties, thermogram, ultrasonic signals, and time-of-flight C-scan image in detail.

The authors thank the financial support from a scholarship from the Ministry of Science and Technology, the Royal Thai Government (ST_4838), as well as from an Advanced Investigator Award from the European Research Council (Biophononics 340117).

AUTHOR DECLARATIONS

Conflict of Interest

The authors have no conflicts to disclose.

Author Contributions

Pracha Yambangyang: Data curation (equal); Formal analysis (equal); Methodology (equal); Validation (equal); Writing – review and editing (equal). **Rab Wilson:** Formal analysis (equal); Methodology (equal); Supervision (equal); Writing – original draft (equal). **Julien Reboud:** Data curation (equal); Formal analysis (equal); Methodology (equal); Validation (equal); Writing – original draft (equal); Writing – review and editing (equal). **Jonathan M. Cooper:** Conceptualization (equal); Funding acquisition (equal); Supervision (equal); Writing – original draft (equal); Writing – review and editing (equal). **Andriejus Demčenko:** Conceptualization (equal); Formal analysis (equal); Investigation (equal); Software (equal); Supervision (equal); Validation (equal); Writing – original draft (equal); Writing – review and editing (equal).

DATA AVAILABILITY

The data that support the findings of this study are openly available in Enlighten at http://doi.org/10.5525/gla.researchdata.1332.

REFERENCES

[1]L. Yu, Adv. Drug Delivery Rev. **48**, 27 (2001).
[2]M. Nouman, J. Saunier, E. Jubeli, and N. Yagoubi, Polym. Degrad. Stab. **143**, 239 (2017).
[3]S. Ramakrishna, J. Mayer, E. Wintermantel, and K. W. Leong, Compos. Sci. Technol. **61**, 1189 (2001).
[4]S. Kahlen, G. Wallner, and R. Lang, Sol. Energy **84**, 1567 (2010).
[5]I. Jakubowicz, N. Yarahmadi, and T. Gevert, Polym. Degrad. Stab. **66**, 415 (1999).
[6]K. F. Makris, J. Langeveld, and F. H. L. R. Clemens, Struct. Infrastruct. Eng. **16**, 880 (2020).
[7]L. C. E. Struik, *Physical Ageing in Amorphous Polymers and Other Materials* (Elsevier Science, 1978).
[8]I. M. Hodge, Science **267**, 1945 (1995).
[9]J. M. Hutchinson, Prog. Polym. Sci. **20**, 703 (1995).
[10]A. V. Iacopi and J. R. White, J. Appl. Polym. Sci. **33**, 577 (1987).
[11]X. Colin, G. Teyssedre, and M. Fois, *Ageing and Degradation of Multiphase Polymer Systems* (John Wiley & Sons, Ltd., 2011), pp. 797–841.
[12]A. Demčenko, R. Akkerman, P. B. Nagy, and R. Loendersloot, NDT & E Int. **49**, 34 (2012).
[13]N. Yarahmadi, I. Jakubowicz, and T. Hjertberg, Polym. Degrad. Stab. **82**, 59 (2003).
[14]B. E. Read, G. D. Dean, P. E. Tomlins, and J. L. Lesniarek-Hamid, Polymer **33**, 2689 (1992).
[15]P. Tiemblo, J. Guzmán, E. Riande, C. Mijangos, and H. Reinecke, Polymer **42**, 4817 (2001).
[16]H. Wang, S. Masters, M. A. Edwards, J. O. Falkinham, and A. Pruden, Environ. Sci. Technol. **48**, 1426 (2014).
[17]L. C. E. Struik, Ann. N.Y. Acad. Sci. **279**, 78 (1976).
[18]V. Bershtein and V. Yegorov, Polym. Sci. USSR **27**, 2743 (1985).
[19]H. H. D. Lee and F. J. M. Garry, J. Macromol. Sci., Part B **29**, 185 (1990).
[20]M. Bosma, B. G. ten, and T. S. Ellis, Macromolecules **21**, 1465 (1988).
[21]A. Nogales and B. B. Sauer, J. Polym. Sci., Part B: Polym. Phys. **36**, 913 (1998).
[22]C. Bauwens-Crowet, J. C. Bauwens, and G. Homès, J. Polym. Sci. Part A-2: Polym. Phys. **7**, 735 (1969).
[23]J. S. Havriliak and T. J. Shortridge, J. Appl. Polym. Sci. **37**, 2827 (1989).
[24]H. Visser, T. Bor, M. Wolters, T. Engels, and L. Govaert, Macromol. Mater. Eng. **295**, 637 (2010).
[25]S. Vyazovkin, N. Sbirrazzuoli, and I. Dranca, Macromol. Chem. Phys. **207**, 1126 (2006).
[26]V. Plaček, J. Therm. Anal. Calorim. **80**, 525 (2005).
[27]K. Jin, L. Li, and J. M. Torkelson, Polymer **115**, 197 (2017).
[28]A. Demčenko, V. Koissin, and V. A. Korneev, Ultrasonics **54**, 684 (2014).
[29]V. A. Korneev and A. Demčenko, J. Acoust. Soc. Am. **135**, 591 (2014).
[30]M. Mazilu, A. Demčenko, R. Wilson, J. Reboud, and J. M. Cooper, Phys. Rev. Lett. **121**, 244301 (2018).

[31]M. H. Skjelvareid, Y. Birkelund, and Y. Larsen, NDT&E Int. **54**, 151 (2013).
[32]F. D. Murnaghan, Am. J. Math. **59**, 235 (1937).
[33]F. P. C. Gomes, W. T. J. West, and M. R. Thompson, Polymer **131**, 160 (2017).
[34]A. Chamas, H. Moon, J. Zheng, Y. Qiu, T. Tabassum, J. H. Jang, M. Abu-Omar, S. L. Scott, and S. Suh, ACS Sustainable Chem. Eng. **8**, 3494 (2020).
[35]M. Ito and K. Nagai, Polym. Degrad. Stab. **92**, 260 (2007).
[36]F. Ania, J. Martínez-Salazar, and F. J. Baltá Calleja, J. Mater. Sci. **24**, 2934 (1989).
[37]B. Liu, H. Xia, G. Fei, G. Li, and W. Fan, Macromol. Chem. Phys. **214**, 2519 (2013).
[38]I. Alig, F. Stieber, S. Wartewig, and G. Fytas, Polymer **29**, 975 (1988).
[39]R. W. Mailen, M. D. Dickey, J. Genzer, and M. A. Zikry, J. Polym. Sci., Part B: Polym. Phys. **55**, 1207 (2017).
[40]K. P. Curra, P. D. Mourad, V. A. Khokhlova, R. O. Cleveland, and L. A. Crum, IEEE Trans. Ultrason. Ferroelectr. Freq. Control **47**, 1077 (2000).
[41]A. Bhargava, K. Peng, J. Stieg, R. Mirzaeifar, and S. Shahab, RSC Adv. **7**, 45452 (2017).
[42]H. Y. Guney, T. Oskay, and H. S. Özkan, J. Polym. Sci. Part B: Polym. Phys. **33**, 985 (1995).
[43]M. Zakeri, S. M. Keller, Y. E. Wang, and C. S. Lynch, New J. Phys. **22**, 023009 (2020).
[44]I. Alig, F. Stieber, and S. Wartewig, Polymer **32**, 2146 (1991).
[45]Y. Zhou and S. T. Milner, Macromolecules **51**, 3865 (2018).
[46]P. Paloniemi and P. Lindstrom, IEEE Trans. Electr. Insul. **EI-16**, 18 (1981).
[47]A. Demčenko, L. Mainini, and V. A. Korneev, Ultrasonics **57**, 179 (2015).
[48]L. J. Broutman and S. M. Krishnakumar, Polym. Eng. Sci. **16**, 74 (1976).
[49]A. Siegmann, A. Buchman, and S. Kenig, Polym. Eng. Sci. **22**, 40 (1982).
[50]A. Demčenko, M. Mazilu, R. Wilson, A. W. F. Volker, and J. M. Cooper, IEEE Trans. Ultrason. Ferroelectr. Freq. Control **65**, 1056 (2018).
[51]J. H. Kang, T. P. Miettinen, L. Chen, S. Olcum, G. Katsikis, P. S. Doyle, and S. R. Manalis, Nat. Methods **16**, 263 (2019).
[52]J. Rufo, F. Cai, J. Friend, M. Wiklund, and T. J. Huang, Nat. Rev. Methods Primers **2**, 30 (2022).
[53]V. Romanov, G. Silvani, H. Zhu, C. D. Cox, and B. Martinac, Small **17**, 2005759 (2021).
[54]A. Ozcelik, J. Rufo, F. Guo, Y. Gu, P. Li, J. Lata, and T. J. Huang, Nat. Methods **15**, 1021 (2018).
[55]P. Zhang, H. Bachman, A. Ozcelik, and T. J. Huang, Annu. Rev. Anal. Chem. **13**, 17 (2020).